ROYAL SOCIETY OF CHEMISTRY

Journal Name

COMMUNICATION

Spatially encoded 2D and 3D diffusion-ordered NMR spectroscopy

Ludmilla Guduff,[a] Ilya Kuprov,[b] Carine van Heijenoort[a] and Jean-Nicolas Dumez[a]*

We show that the acquisition of 3D diffusion-ordered NMR spectroscopy (DOSY) experiments can be accelerated significantly with the use of spatial encoding (SPEN). The SPEN DOSY approach is discussed, analysed with numerical simulation, and illustrated on a mixture of small molecules.

The analysis of complex mixtures of small molecules is a major challenge in chemistry, with applications in metabolomics, natural-product research and chemical synthesis. Nuclear magnetic resonance (NMR) spectroscopy is a powerful tool to address this challenge; arrays of NMR spectra are commonly used for identification and structure elucidation. A variety of schemes have been reported to recover the "pure" spectra of components in mixtures.[1] Diffusion-ordered spectroscopy (DOSY) is the most widely used approach for such spectral separation.[2] In DOSY, signal amplitudes are attenuated by a pair of gradient pulses (each of area K) separated by a diffusion delay; a fit of the diffusion-induced decay returns the diffusion coefficient D for each resonance, so that sub-spectra can be separated according to the value of D.

The DOSY approach is applicable to a range of N-dimensional (ND, with N typically 1 or 2) NMR experiments.[2a, 3] The use of an incremented gradient area, however, results in a pseudo-(N+1)D experiment and increases the total experimental time by a factor of about 10. Several strategies have been described for the acceleration of DOSY experiments. The original HR-DOSY pulse sequence requires multiple steps of phase cycling, which may be reduced to one with the *Oneshot* approach.[4] The number of gradient increments can be reduced, using a non-uniform sampling of the diffusion dimension.[5] For 3D DOSY, the diffusion

information may also be encoded in the width of the NMR peaks, with the accordion approach.[6] Single-scan DOSY implementations include the *Difftrain* approach,[7] which has found applications for the analysis of heterogeneous media. Alternatively, the acquisition of the DOSY data may be parallelised, with a spatial encoding of the K dimension.[8] This concept, introduced by Keeler and co-workers, makes it possible to acquired 2D DOSY data in a single scan. It is particularly useful for the analysis of transient processes and hyperpolarised samples.[9]

In this communication, we show that spatially encoded diffusion-ordered spectroscopy (SPEN DOSY) can be used for fast separation of 2D correlation spectra of components in mixtures. In order to gain insight into the SPEN DOSY mechanism, we first introduce a numerical simulation framework that can simultaneously account for the complex spin and spatial dynamics. We then describe a generalised implementation of SPEN DOSY. As an example of SPEN 3D DOSY, the acquisition of a 3D DOSY COSY spectrum is accelerated by over an order of magnitude.

Figure 1a shows a schematic pulse sequence for spatially encoded multidimensional DOSY experiments. The gradient pulses of the classic STE-based DOSY pulse sequence are replaced with the concurrent application of linearly swept chirp pulses and magnetic field gradients.[8b] The first chirp and gradient pair imparts a spatially dependent phase, which may be approximated as[10]

$$\varphi(z) = -\gamma G_e T_e \frac{z^2}{L} + \gamma G_e T_p z, \qquad \text{Eq. 1}$$

where T_e is the duration of the chirp pulse, G_e is the amplitude of the encoding gradient, L is the length of the region swept by the pulse, T_p is the duration of the post-chirp gradient. The spatial derivative of the phase, which corresponds to the effective gradient area, is thus position-dependent, with

$$K(z) = -2\gamma G_e T_e \frac{z}{L} + \gamma G_e T_p. \qquad \text{Eq. 2}$$

In the absence of diffusion, the second chirp and gradient pair would fully compensate the phase imparted by the first one. The attenuation caused by translational diffusion may be expressed as:[8b, 8c]

$$S(z) = S_0 \exp(-D\Delta'(K(z))^2), \qquad \text{Eq. 3}$$

where D is the diffusion coefficient of the molecule and Δ' is an effective diffusion delay. Equations 2 and 3 reveal the spatial dependence of the local diffusion weighting, which may be seen as a parallel encoding of all DOSY sub-experiments.
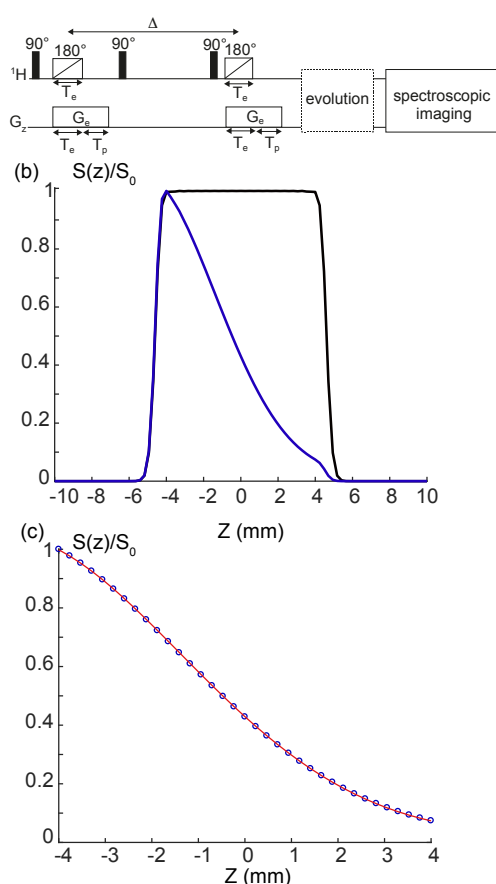

Fig. 1 Spatially encoded diffusion-ordered spectroscopy. (a) Schematic SPEN DOSY pulse sequence; Δ is the time that elapses between the centres of the chirp pulses. (b) Simulated 1D MR image of a sample after the SPEN DOSY pulse sequence with (blue) and without (black) translational diffusion with $D = 8 \times 10^{-10}$ m^2.s^{-1}. (c) Diffusion decay curves extracted from the 1D MR image, shown together with the best-fit curve obtained using a modified Stejskal-Tanner equation (Eq. 3), which yields $D = 7.98 \times 10^{-10}$ m^2.s^{-1}. A model that neglects diffusion during the chirp yields $D = 7.86 \times 10^{-10}$ m^2.s^{-1}. A model that assumes an instantaneous flip during the chirp yields $D = 7.82 \times 10^{-10}$ m^2.s^{-1}.

In SPEN DOSY, the diffusion information for each resonance is recovered at the acquisition stage by acquiring an "image" of the sample with magnetic resonance imaging (MRI) methods.[8b, 8c] Since DOSY is applied to samples with multiple resonances, fast spectroscopic imaging is mandatory for single-scan implementations. Here we use the echo-planar-spectroscopic imaging approach (EPSI), of the kind employed in ultrafast 2D NMR.[10] As illustrated in Fig. 1a, an evolution block can be included in the SPEN DOSY pulse sequence to yield an accelerated 3D DOSY experiment.

While the concept of spatially encoded diffusion NMR experiments was introduced some time ago,[8a, 8b] investigations into the properties of the SPEN DOSY approach were made difficult by the challenge of describing the underlying spin dynamics together with the diffusion process. The recent development of a numerical simulation framework that

seamlessly integrates spin and spatial variables makes it possible to describe SPEN DOSY in a computationally efficient manner.[11] With this approach, based on the Fokker-Planck formalism, the validity of the approximations can be explored, together with possible sources of artefacts and ways to correct them. Figure 1b shows the simulated data set obtained for an ensemble of uncoupled spins subjected to the SPEN DOSY pulse sequence; the acquisition is a simple gradient echo. In the absence of diffusion, the spatial profile is determined by the selectivity profile of the smoothed chirp pulse. When the diffusion operator is included in the simulation, the spatial profile reveals the diffusion decay curve. The region corresponding to the plateau of the chirp selectivity profile can then be used for modelling the data.

Numerical simulation here serves to improve the model used to fit the data (see the SI for the description of each model). The model used by Frydman and co-workers and Valette and co-workers[8c, 12] accounts for diffusion during the chirp, but with an approximate expression for $K(z)$. In contrast, the model used by Keeler and co-workers[8b] relies on an exact calculation of the phase imparted by the chirp but neglects diffusion during the chirp. Either model results in a small but systematic error. By using a modified equation, with $K(z)$ given by the exact expression and an effective diffusion time $\Delta' = \Delta - (T_e + T_p)/2$, the systematic error becomes negligible, as shown in Fig. 1c. Further numerical investigations will be described in detail elsewhere.

The proposed implementation of SPEN 2D DOSY is shown in Fig. 2a. The post-chirp gradient makes it possible to encode a larger range of effective gradient area. In addition to the gradients for spatial encoding and imaging, pairs of crusher gradient pulses are used around the chirp pulses, as well as for the selection of the anti-echo pathway. Further gradient pulses include a spoiler pulse during longitudinal storage, as well as compensating pulses that yield a null total gradient area before acquisition. When a triple-axis gradient probe is available, as for the experiments reported here, coherence pathway selection and spatial encoding may be achieved along orthogonal axes, resulting in a simpler implementation.

The properties of the SPEN 2D DOSY pulse sequence may be illustrated with a model mixture of small molecules, which consists of alcohols of varying chain length (methanol, ethanol and propanol) and an amino acid (L-valine). Fig. 2b shows the spectroscopic imaging data obtained on this model mixture. For each resonance, the spatial profile is obtained as slice of the data matrix; the DOSY decay curve then corresponds to the region swept by the chirp pulse, shown in Fig. 2c. A reference profile, obtained with a sample of H_2O/D_2O, may be used to account for spatial non-uniformity (i.e., the S_0 term in Eq. 2). The classic DOSY processing (single-exponential fit to Eq. 3) may be applied to this SPEN data set resulting in the DOSY display shown in Fig. 2d. For this mixture, a very good separation of all the components is achieved. This separation is obtained in a single scan of less than 250 ms, which may be compared with the 17 min required by the conventional experiment. The acceleration results from both the choice of coherence selection gradients, which removes the need for

COMMUNICATION

phase cycling (as in the *Oneshot* pulse sequence), and the use of spatial encoding, which removes the need for incremented
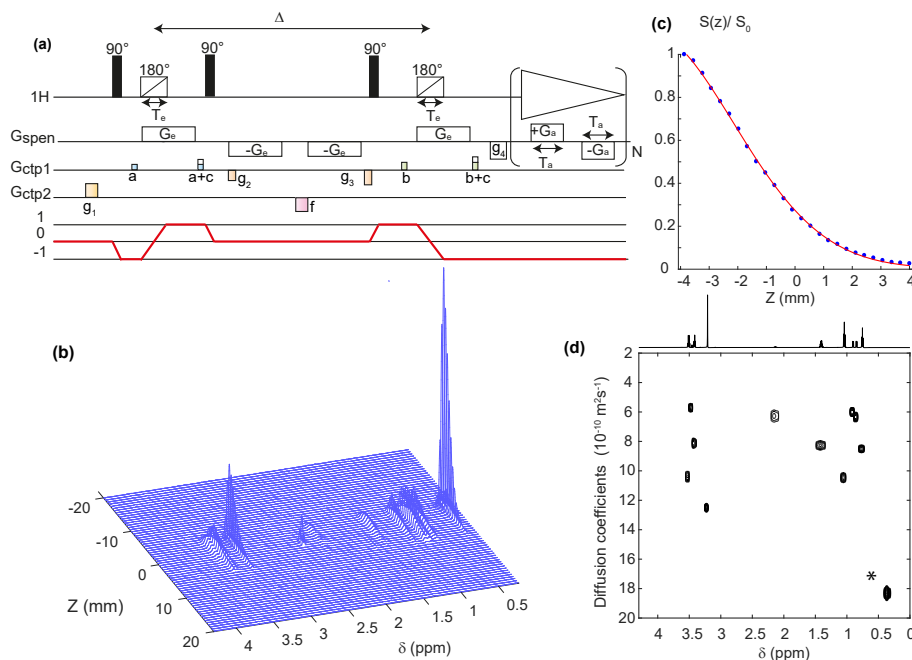
gradient areas.

Fig. 2 SPEN 2D DOSY. (a) Pulse sequence for SPEN 2D DOSY. The selected coherence transfer pathway is shown in red. Gradients *a* and *b* are crushers surrounding the refocusing chirp pulses; gradient *c* selects the anti-echo pathway for the stimulated echo; gradient *f* is a spoiler during longitudinal storage; g_1, g_2 and g_3 are compensating gradients. (b) 2D spectroscopic imaging data set obtained with the SPEN 2D DOSY experiment on a mixture of 3 alcohols (methanol, ethanol, propanol) and an amino-acid (L-valine), at a concentration of ~100 mM in D_2O. (c) Diffusion decay curve obtained from the data set shown in (b), for the methanol CH_3 resonances at 3.2 ppm. The best fit-curve for the modified Stejskal-Tanner equation is shown in red with $D = 12.5 \times 10^{-10}$ m².s⁻¹ (d) 2D DOSY display obtained from the data set shown in (b), the average diffusion coefficients are 18.4×10^{-10} m².s⁻¹ for water, 12.5×10^{-10} m².s⁻¹ for methanol, 10.3×10^{-10} m².s⁻¹ for ethanol, 8.5×10^{-10} m².s⁻¹ for propanol and 6.1×10^{-10} m².s⁻¹ for L-valine. The water peak is folded and indicated by an asterisk. The ¹H pulse-acquire spectrum is shown above the DOSY display. The experiment was carried out with a 600 MHz spectrometer equipped with a triple-axis gradient high-resolution probe.

The concept of diffusion-ordered spectroscopy is also applicable to a large range of multidimensional experiments.[2a, 3] Additional spectroscopic dimensions help resolving signal overlaps, which are detrimental to the determination of diffusion coefficients. It may also provide further structural information. The concept of SPEN DOSY may be extended to such multidimensional experiments. While not single-scan, the resulting experiments will still be significantly faster than conventional ones. A first demonstration of the proposed SPEN 3D DOSY concept is given here with the SPEN DOSY COSY experiment. Figure 3a shows the corresponding pulse sequence, which is obtained by appending an incremented evolution delay and a mixing RF pulse to the SPEN 2D DOSY experiment. With this approach, the entire 3D data set is obtained within a total experimental time of 12 min, which is significantly shorter than the 14 hours needed for the conventional experiments After suitable data rearrangement and processing, diffusion-ordered spectra are obtained. On the model mixture of alcohols, the SPEN DOSY COSY experiment achieves a good separation of all spectra, as shown in Fig. 3b-g.

The choice of encoding and acquisition parameters has to account for several parameter relations and hardware constraints. The spectral width of the spectroscopic acquisition dimension is given by the inverse of the period of the acquisition gradient trains. Resonances outside that range will undergo folding and may thus still be recovered, as is the case

with the water peak in Figs 2 and 3. Alternatively, selective excitation pulses may be used to prevent such folding. The resolution in the spectroscopic dimension is constrained here by the gradient hardware, which cannot sustain EPSI acquisitions of more than ~150 ms for the required gradient strength and switching rates. The resulting resolution is commonly found to be sufficient for the analysis of mixtures with ultrafast 2D NMR experiments.[13]

In its present form, the SPEN DOSY approach provides a good separation of components in the mixture. While the relative order of the diffusion coefficients is retrieved, their value is still subjected to systematic errors; the accuracy of SPEN DOSY is not equivalent to that of the conventional approach. Diffusion coefficients separated by less than 0.5×10^{-10} m².s⁻¹ are also found to be difficult to separate. Improvements will be obtained by accounting for sources of systematic errors, including temperature regulation parameters, gradient non-linearity and RF inhomogeneity. Improved results would also be obtained with more stable gradients. Investigations along these lines are in progress.

In summary, we have shown that spatially encoded diffusion ordered spectroscopy is a general tool for the separation of 1D and 2D spectra of components in a mixture. We introduce a powerful numerical tool for the simulation, understanding and improvement of SPEN DOSY experiments. Building on earlier work, we propose a robust implementation

COMMUNICATION   Journal Name

of the SPEN 2D DOSY approach. We finally show that 3D DOSY experiments can be accelerated significantly, using a spatial encoding of the diffusion dimension. The resulting tools will be useful for the analysis of time-evolving processes, such as chemical reactions and hyperpolarised samples.
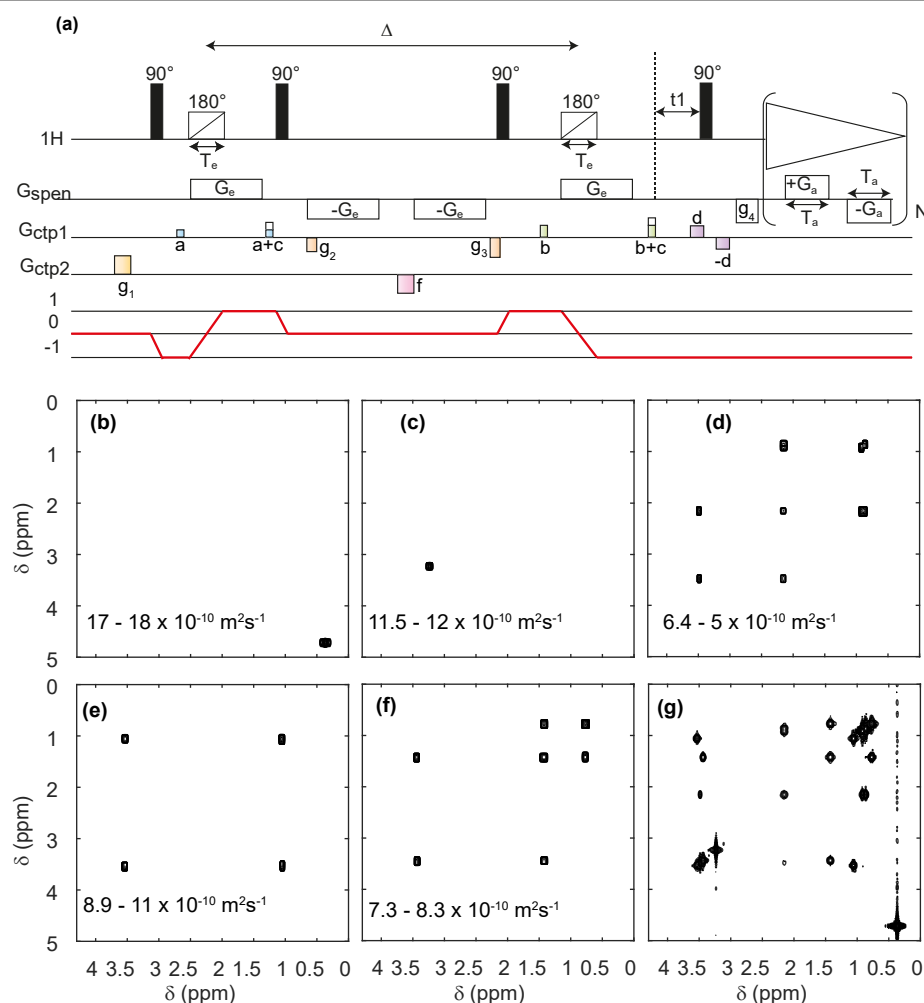
Fig. 3 SPEN 3D DOSY. (a) Pulse sequence for SPEN COSY DOSY. (b-f) COSY-type spectra obtained as slabs of the 3D (D, δ_{direct}, $\delta_{indirect}$) dataset resulting from DOSY processing. The selected range in D is shown in each panel. The slice of the (z, δ_{direct}, $\delta_{indirect}$) dataset with the lowest diffusion gradient area is shown in (g). The experiment was carried out with a 600 MHz spectrometer equipped with a triple-axis gradient high-resolution probe.

Notes and references

1   (a) S. W. Wei, J. Zhang, L. Y. Liu, T. Ye, G. A. N. Gowda, F. Tayyari and D. Raftery, *Anal. Chem.*, 2011, **83**, 7616; (b) I. Toumi, B. Torresani and S. Caldarelli, *Anal. Chem.*, 2013, **85**, 11344; (c) P. Lameiras and J. M. Nuzillard, *Anal. Chem.*, 2016, **88**, 4508; (d) F. Zhang and R. Brueschweiler, *Angew. Chem. Int. Ed.*, 2007, **46**; (e) A. A. Colbourne, G. A. Morris and M. Nilsson, *J. Am. Chem. Soc.*, 2011, **133**.

2   (a) C. S. Johnson, *Prog. Nucl. Magn. Reson. Spectrosc.*, 1999, **34**, 203; (b) H. Barjat, G. A. Morris, S. Smart, A. G. Swanson and S. C. R. Williams, *J. Magn. Reson., Ser B*, 1995, **108**, 170.

3   (a) J. M. Newman and A. Jerschow, *Anal. Chem.*, 2007, **79**, 2957; (b) M. Nilsson, A. M. Gil, I. Delagadillo and G. A. Morris, *Chem. Commun.*, 2005, 1737; (c) S. Viel and S. Caldarelli, *Chem. Commun.*, 2008, 2013.

4   M. D. Pelta, G. A. Morris, M. J. Stchedroff and S. J. Hammond, *Magn. Reson. Chem.*, 2002, **40**, S147.

5   M. Urbanczyk, W. Kozminski and K. Kazimierczuk, *Angew. Chem. Int. Ed.*, 2014, **53**, 6464.

6   S. M. Pudakalakatti, K. Chandra, R. Thirupathi and H. S. Atreya, *Chem. Eur. J.*, 2014, **20**, 15719.

7   J. P. Stamps, B. Ottink, J. M. Visser, J. P. M. van Duynhoven and R. Hulst, *J. Magn. Reson.*, 2001, **151**, 28.

8   (a) N. M. Loening, J. Keeler and G. A. Morris, *J. Magn. Reson.*, 2001, **153**, 103; (b) M. J. Thrippleton, N. M. Loening and J. Keeler, *Magn. Reson. Chem.*, 2003, **41**, 441; (c) Y. Shrot and L. Frydman, *J. Magn. Reson.*, 2008, **195**, 226.

9   S. Ahola, V. V. Zhivonitko, O. Mankinen, G. Zhang, A. M. Kantola, H.-Y. Chen, C. Hilty, I. V. Koptyug and V.-V. Telkki, *Nature Communications*, 2015, **6**, 8363.

10   A. Tal and L. Frydman, *Prog. Nucl. Magn. Reson. Spectrosc.*, 2010, **57**, 241.

11   (a) H. J. Hogben, M. Krzystyniak, G. T. P. Charnock, P. J. Hore and I. Kuprov, *J. Magn. Reson.*, 2011, **208**, 179; (b) I. Kuprov, *J. Magn. Reson.*, 2016, **270**, 124.

12   J. Valette, F. Lethimonnier and V. Lebon, *J. Magn. Reson.*, 2010, **205**, 255.

13   P. Giraudeau and L. Frydman, *Annu. Rev. Anal. Chem.*, 2014, **7**, 129.